SUPPORTING INFORMATION

Modulation of Charge Transfer Exciton Dynamics in Organic Semiconductors Using Different Structural Arrangements

Cristian Soncini,[a] Abhishek Kumar,[b] Federica Bondino,[a] Elena Magnano,[a,c] Matija Stupar,[d] Barbara Ressel,[d] Giovanni De Ninno,[d,e] Antonis Papadopoulos,[f] Efthymis Serpetzoglou,[f] Emmanuel Stratakis,[f] and Maddalena Pedio[a]*

[a]*Istituto Officina dei Materiali, Consiglio Nazionale delle Ricerche, Trieste, Italy.*

[b] *Department of Physics, Chandigarh University, Chandigarh, India.*

[c] *Department of Physics, University of Johannesburg, Johannesburg, South Africa.*

[d]*Laboratory of Quantum Optics, University of Nova Gorica, Ajdovščina, Slovenia.*

[e] *Elettra - Sincrotrone Trieste S.C.p.A, Trieste, Italy.*

[f] *FORTH Institute of Electronic Structure and Laser Foundation for Research and Technology Hellas and University Of Crete, Hellas.*

Corresponding Author

*cristian.soncini@ifn.cnr.it

Methods

The cobalt phthalocyanine (CoPc), β-form powder, was purchased from Sigma Aldrich, dye content of 97%. CoPc deposition was performed by thermal sublimation from resistively heated quartz crucibles in ultrahigh vacuum UHV conditions ($<10^{-9}$ mbar). CoPc thin films were grown onto three different substrates, Au(111), graphene (Gr) and ITO. Before the deposition, the Au(111) surface was reconstructed by several Ar sputtering and annealing cycles in UHV. The Gr substrate was produced by the polymer transfer method of commercial Gr, purchased from Graphenea S.A., on a bulk Si wafer. The ITO surface was rinsed using acetone and distilled water. The CoPc film growth was performed at a low deposition rate of 2 Å min^{-1}. The film thickness was measured via oscillating quartz microbalance after a degassing of the source at T lower than the sublimation temperature, obtaining CoPc films of 24±2 nm nominal thickness.

Near edge X-ray absorption fine structure spectroscopy (NEXAFS) of the Co $L_{2,3}$ edge as a function of the X-ray incidence angle was performed in fluorescence mode (using a micro-channel plate, Hamamatsu F4655-13) at the BACH beamline of Elettra synchrotron in Trieste, Italy.

PES and TR-PES measurements were performed at the "Laboratory of quantum optics" of CITIUS in Nova Gorica. The PES spectra were obtained using a commercial Ti:Sa laser source (Coherent, Legend Elite Duo), from which high-order harmonics were generated and monochromatized. HH35 ($h\upsilon \approx 38.5$ eV) was selected: the overall resolution of the probe beam was 130 meV. The excitation (pump) pulses were generated from an OPA (Coherent OPerA) set at 610 nm (2.0 eV), delivering on the sample 1 mJ cm^{-2}. TR-PES measurements were performed using an R3000 hemispherical electron energy spectrometer from VG-Scienta.

The IPES measurements were performed using a homemade Erdman-Zipf electron gun that provides a highly collimated electron beam at the SIPE laboratory, CNR-IOM in Trieste. The electron beam divergence was ~2°. Photons emitted by the sample were collected by a homemade Geiger-Müller type detector with a He-I_2 gas mixture and an SrF_2 entrance window filtering photons of energy $h\nu$=9.5 eV. The experimental resolution was 0.25 eV, as measured by the Fermi level (E_F) onset of a clean Ta foil. The IPES spectra were normalized at each point to the incident electron beam current.

TAS measurements in the Vis/IR range (from 1.12 eV to 2.34 eV) were performed at the "Ultrafast Laser Micro and Nano processing" laboratory of the Foundation for Research and Technology – Hellas research facility in Crete, Hellas. The Femtosecond laser pulses were generated using a (Yb:KGW) femtosecond laser source with a pulse duration of 170 fs, 1 kHz repetition rate, and 1.21 eV of fundamental wavelength. The beam was split into a pump and a probe beam. An OPA was used to select photon energies of 1.21 eV, 2.41 eV and 3.1 eV for the pump pulses. For the probe pulses, a supercontinuum white light in the 1.12 eV to 2.34 eV range of wavelengths was generated using a YAG crystal. The time resolution was 250 fs. The experiments were performed either in reflection or transmission geometry mode in the 15 ps and the 7 ns time domains. The differential spectra of the three samples were obtained according to the equation:

$$\Delta OD = -\log\left(\frac{I(t)}{I_0}\right) \qquad \text{(S1)}$$

where I(t) and I_0 are the detected probe intensity signal with and without sample excitation by pump pulse, respectively.

The decay time for specific probe energy was obtained fitting the ΔOD decay curves as function of the time delay by a mono or multi-exponential function according to:

$$\Delta OD = \sum_n A_n e^{-\frac{t}{\tau_n}} + C \qquad \text{(S2)}$$

where A_n and τ_n are the contributions and lifetimes of the exponential decay, and C is a constant value which describes a slower dynamics in a time range that is too long to be measurable in the experimental time window used.

S1. Structural characterization of the ordered thin films

An effective way to control the molecular orientation and obtain different film structures is to exploit the templating effect using different substrates. As demonstrated by ref. 1 it is possible to grow a specific molecular arrangement avoiding the admixture of the ordered phases. Scanning tunnel microscopy studies have shown that the first CoPc layer adopts a square or a hexagonal lattice when grown on Gr or Au(111) respectively[2-4], leading to different molecular stacking for subsequent layers depositions. In this way, we have grown thin films with predominant herringbone or brickwork-based structures on Gr or Au(111) substrates, respectively. The CoPc/Au(111) film is a co-facial CoPc stacking based on a brickwork pattern. In the following, we use the term "brickwork" to denote the CoPc/Au(111) film. CoPc deposition on ITO leads to a disordered film[5].

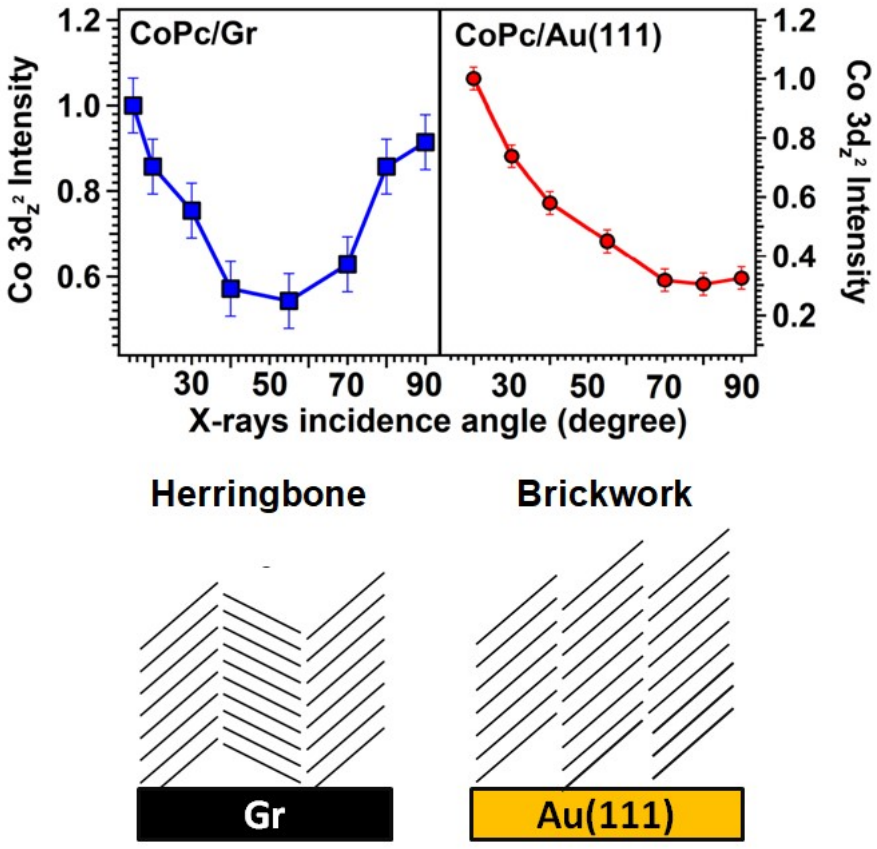

Figure S1. *Dependence of the Co3d$_{z^2}$ peak intensity as a function of the X-ray incidence angle of the CoPc/Gr and CoPc/Au(111) samples.*

The characterization of the molecular structure in the CoPc/Gr and CoPc/Au(111) samples has been carried out by exploiting the polarization dependence of the out-of-plane Co $3d_z^2$ orbital of the CoPc. Its assignment as the first resonance peak of the Co L_3 XAS was known from literature[6] . Figure S1 shows the polarization dependence of the Co $3d_z^2$ peak intensity as a function of the X-ray incidence angle as measured by Co L_3 XAS. A well-defined molecular orientation is confirmed in both cases, though the two trends strongly differ. The monotonous decrease of the Co $3d_z^2$ intensity in the CoPc/Au(111) sample suggests a brickwork structure, whereas the symmetric trend in the CoPc/Gr sample indicates a herringbone structure.

S2. Peak position evaluation of PES and IPES spectra

In PES and IPES spectra several factors affect the energy level positions[7 and refs therein]. Peak broadening is due to the instrumental resolution, limited angular resolution and inelastic scattering processes. Peaks can be slightly shifted in energy because of the incomplete screening of holes/electrons induced in the system during the measurement and by polarization energy induced by molecular cations and anions originated during PES and IPES measurements.

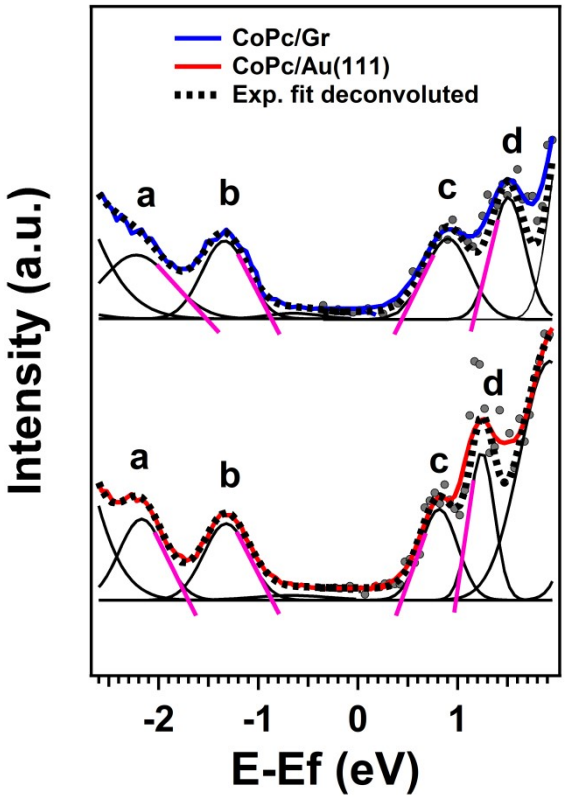

Figure S2. *Schematic of the procedure used for the determination of the peak edges from PES and IPES spectra. In the IPES spectral region the dots are the measured data and the continuous line (blue and red) the best fit obtained without deconvolution with the instrumental broadening. The fit*

components (continuous black curves) are those obtained after deconvolution and the dashed line the respective deconvoluted experimental fit.

As a consequence, the spectral weight with lower binding energy corresponds to the best approximation of the ground state properties of the sample, and the energy level positions in PES and IPES spectra are better represented by the edges of the peaks[7]. The edges (determined from linear extrapolation) and the related fit of the peak a, b, c and d after deconvolution of the experimental resolution are shown Figure S2. Due to the high PES experimental resolution (130 meV) the deconvoluted fit of the PES spectra do not show significant fit improvement with respect to the experimental data.

Sample	Peak a	Peak b	Peak c	Peak d	b-d energy gap (HOMO-LUMO)	b-c energy gap (HOMO- a_{1g})
CoPc/Gr	-2.20 eV	-1.30 eV	0.90 eV	1.50 eV	2.00 eV	1.30 eV
CoPc/Au(111)	-2.15 eV	-1.30 eV	0.85 eV	1.35 eV	1.85 eV	1.30 eV

Table S1: *Summary of the peak edges obtained by linear extrapolation from the PES and IPES data of the peaks a, b, c and d of the two samples and the estimated b-d and b-c energy gaps (edge-to-edge).*

Table S1 summarizes the edge values obtained and the estimated b-d and b-c energy gaps in the two samples (the peaks b, c and d are assigned to the HOMO, a_{1g} (unoccupied) and LUMO respectively, see the main text for more details).

S3. Thin film damaging

Figure S3 shows the CoPc/Au(111) VB spectra as a function of the irradiation time by using 38 eV photon energy. The spectrum just after irradiation (3 min) is the one reported in the combined PES-IPES spectra of the main text. Broadening of the HOMO peak, together with the smearing of the HOMO-1 induced by radiation damage, start to be effective after half an hour of measurements. Since the photon energy is smaller than the Co 3p ionization energy (~55 eV), the observed changes in the peaks should not be originated from the partial dissociation of the CoPc molecule, but more likely from a higher molecular disorder induced by the photon flux.

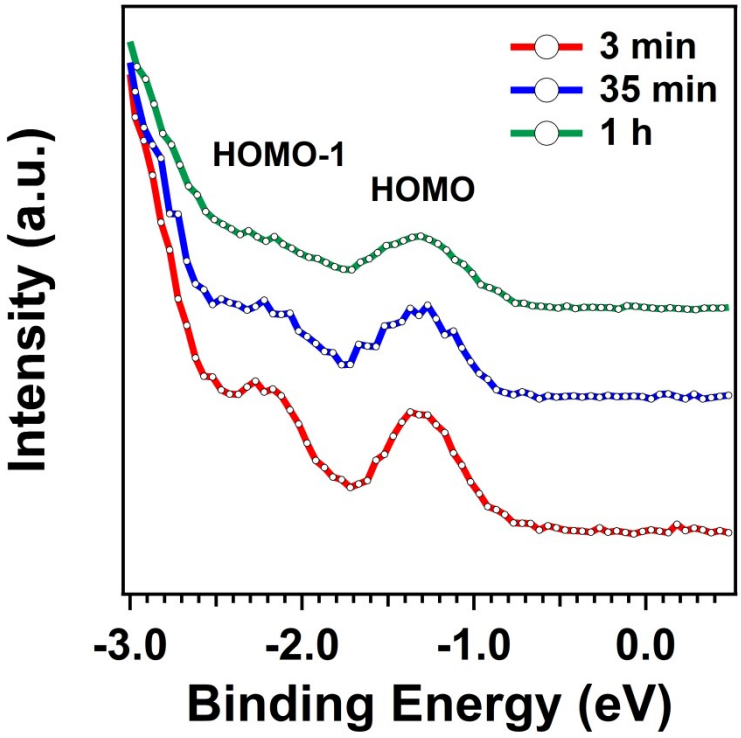

Figure S3. *the CoPc/Au(111) VB spectra as a function of the irradiation time by using 38 eV of photon energy.*

We also investigated the possible degradation and charging of the samples during IPES measurements. The sample's degradation starts to be effective at about 1 hour of acquisition time, observing a broadening and slight decrease in the intensity of the Co3d$_{z^2}$ feature. Within 2 hours, the intensity of the Co3d$_{z^2}$ peak drastically reduces, and the features show energy shifts of about 500 meV toward lower binding energies. To avoid such effects the reported IPES spectra were acquired in a "short" energy range (minimizing the acquisition time to half an hour) and by changing the sample's region scan-by-scan. To ensure a better screening within the penetration depth of the electron beam of the IPES (a few nm) and minimize the sample's charging, the surface of the CoPc films was directly put in contact with a metal pin. Layer-by-layer scans of CoPc films with thicknesses from 5 nm to 40 nm show changes in energy of the IPES features lower than the experimental resolution (< 250 meV).

S4. CoPc/ITO TAS spectra in the ns time domain

Additional TAS measurements of the CoPc/ITO film, in the ns time domain, by using a 2.41 eV pump pulse were performed to clarify the evolution in time of the residual differential signals (still present after 15 ps of time delay) of the bands I, II and III. Figure S4 show that, in all cases, the complete band relaxation is not achieved also within 7 ns showing almost flat decay curves (no significant relaxation occurs in this timescale).

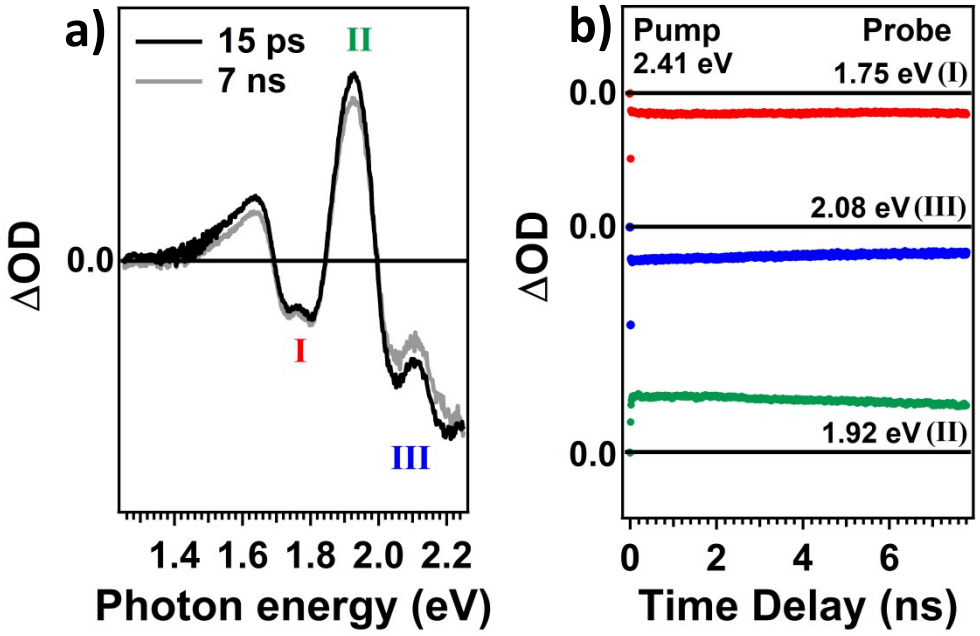

Figure S4. a) *CoPc/ITO film TAS spectra at time delay of 15 ps and 7 ns;* **b)** *Decay curves of the transient band I,II and III using a 2.41 eV pump pulse.*

In the case of the induced absorption signal, namely II, it is a distinctive feature of a relaxation process of triplet states (the relaxation to the singlet ground state has forbidden character and occurs in a long timescale)[8]. On the other hand, the complete band relaxation to the ground state of the bleaching signals I and III (singlet excited states) should occur in a much faster timescale (S→S transition is an allowed character process), implying that the complete relaxation of the singlet excited state to the ground state is not achieved by internal conversion. Since no fluorescence or phosphorescence is reported in the literature for the CoPc[9], non-radiative relaxation through the triplet states is involved. It can be concluded that no further relaxation of singlet states occurs as long as the population of triplet states decays and de-excitation through the triplet states is one of the main relaxation channels in the CoPc thin film.

S5. Relaxation dynamics of H' in the CoPc/Gr and CoPc/Au(111) samples

Figure S5 shows the comparison between the decay curve of H' of the CoPc/Gr sample and the decay curve of the dynamics observed in the bare Gr substrate at the same photon energy of H' (1.27 eV). The relaxation dynamics are identical. Therefore, in the CoPc/Gr case the origin of H' is due to the long-living dynamics of the Gr substrates and not to the molecular film.

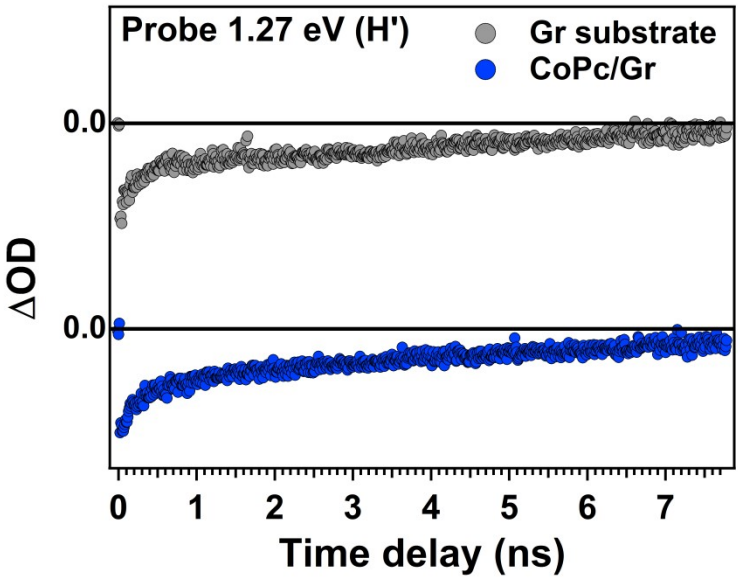

Figure S5 *Comparison between the decay curves at 1.27 eV of photon energy of the CoPc/Gr sample and Gr substrate.*

S6. Herringbone and brickwork crystal structure of α-CoPc crystals

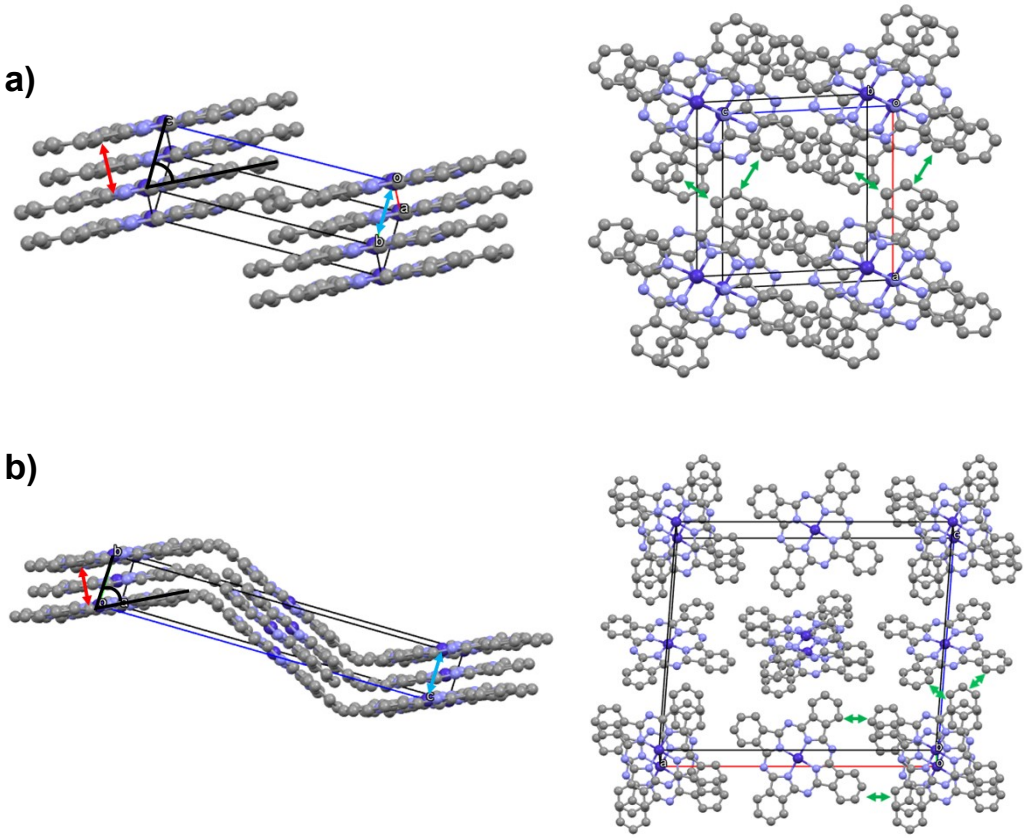

Figure S6. *Side and top view of the* **a)** *brickwork α-CoPc unit cell and* **b)** *herringbone α-CoPc unit cell. The atoms are color coded, i.e., Co is in blue, C is in gray and N is in light blue. The double-headed arrow show the inter-plane distance (red), Co-Co distance (light blue) and the edge-to-edge distance (green). The black lines define the stacking angle. The sliding angle is shown in Figure 5 of the main text.*

Lattice parameter	CoPc	
	brickwork[10]	herringbone[11]
Co-Co distance (Å)	3.75(4)	3.75(0)
Inter-plane distance (Å)	3.42(5)	3.40(6)
Edge-to-edge distance (Å)	3.5-4	3.5-4
Stacking angle (°)	65.8	65.3
Sliding angle (°)	86.2	53.1

Table S2. *Summary of the brickwork and herringbone lattice parameters reported from literature[10,11].*

References:

1 A. C. Cruickshank, C. J. Dotzler, S. Din, S. Heutz, M. F. Toney and M. P. Ryan. The Crystalline Structure of Copper Phthalocyanine Films on ZnO(1-100). *J. Am. Chem. Soc.* **2012**, 134, 14302−14305.

2 P. Järvinen, S. K. Hämäläinen, K. Banerjee, P. Häkkinen, M. Ijäs, A. Harju, and P. Liljeroth. Molecular Self-Assembly on Graphene on SiO_2 and h-BN Substrates. *Nano Lett.* **2013**, 13, 3199−3204.

3 R. A. Rehman, H. J. Zhang, A. Razaq, S. M. Ramay, M. Hasan, M. A. Javed, and S. Atiq. Spectromicroscopy characterization of CoPc-Au(111) interface. *Physica E: Low-dimensional Systems and Nanostructures* **2021**, 125, 114357.

4 D. E. Barlow, L. Scuderio, and K. W. Hipps. Scanning Tunneling Microscopy Study of the Structure and Orbital-Mediated Tunneling Spectra of Cobalt(II) Phthalocyanine and Cobalt(II) Tetraphenylporphyrin on Au(111): Mixed Composition Films. *Langmuir* **2004**, 20, 4413.

5 A. Kumar, D. Naumenko, L. Cozzarini, L. Barba, A. Cassetta, and M. Pedio. Influence of substrate on molecular order for self-assembled adlayers of CoPc and FePc. *J. Raman Spectrosc.* **2018**, 49, 1015-1022.

6 M. G. Betti, P. Gargiani, R. Frisenda, R. Biagi, A. Cossaro, A. Verdini, L. Floreano, and C. Mariani. Localized and Dispersive Electronic States at Ordered FePc and CoPc Chains on Au(110). *J. Phys. Chem. C* **2010**, 114, 21638–21644.

7 D. R. T. Zahn, G. N. Gavrila, and G. Salvan. Electronic and Vibrational Spectroscopies Applied to Organic/Inorganic Interfaces. Chem. Rev. 2007, 107, 1161-1232.

8 A. Gadalla, J. B. Beaufrand, M, Bowen, S. Boukari, E. Beaurepaire, O. Crégut, M. Gallart, B. Honerlage and P. Gilliot, *J. Phys. Chem. C* **2010**, 114, 17854–17863.

9 H. Isago. Optical Spectra of Phthalocyanines and Related Compounds. *Springer: Tokyo*, **2015**.

10 P. Ballirano, R. Caminiti, C. Ercolani, A. Maras and M. A. Orrù. X-ray Powder Diffraction Structure Reinvestigation of the R and â Forms of Cobalt Phthalocyanine and Kinetics of the α→β Phase Transition. *J. Am. Chem. Soc.* **1998**, 120, 12798-12807.

11 M. Ashida, N. Uyeda and E. Suito. Unit cell metastable-form constants of various phthalocyanine. *Bull. Chem. Soc. Jpn.* **1966**, 39, 2616.